Egyptian Journal of Aquatic Biology & Fisheries
Zoology Department, Faculty of Science,
Ain Shams University, Cairo, Egypt.
ISSN 1110 – 6131
Vol. 29(4): 1541 – 1568 (2025)
www.ejabf.journals.ekb.eg

Nanoparticles as a Novel Strategy for Controlling Lernaeosis in the Common Carp (*Cyprinus carpio*)

Asmaa Edrees[1], Nema S. Shaban[2], Reem M. Ramadan[3], Mai A. Salem[3], Faten F. Mohammed[4] and Olfat A. Mahdy[3]

[1]Department of Fish Diseases and Management, Faculty of Veterinary Medicine, Beni-Suef University, PO Box, 62511, Beni-Suef, Egypt
[2]Department of Pharmacology, Faculty of Veterinary Medicine, Beni-suef University, PO Box, 62511, Beni-Suef, Egypt
[3]Department of Parasitology, Faculty of Veterinary Medicine, Cairo University, Egypt
[4]Department of Pathology, College of Veterinary Medicine, King Faisal University, Al-Ahsa, Saudi
*Corresponding Author: asmaaedrees86@yahoo.com

ARTICLE INFO

Article History:
Received: May 20, 2025
Accepted: July 18, 2025
Online: July 24, 2025

Keywords:
Lernaea cyprinacea, *Cyprinus carpio*, Nanotechnology, Control, Immunological response

ABSTRACT

Parasitic diseases, particularly those caused by *Lernaea cyprinacea*, continue to pose a significant challenge to freshwater aquaculture, especially in developing countries, leading to substantial economic losses and impacting fish health and productivity. The present study aimed to develop and evaluate a novel therapeutic approach using zinc–aluminum layered double hydroxide nanocarriers loaded with curcumin (Zn Al LDH-nanocurcumin; ZALDH-NC) to combat *L. cyprinacea* infestations in *Cyprinus carpio* fingerlings. A total of 120 infected fish were divided into four groups and treated with commercial curcumin, Zn Al LDH, Zn Al LDH-nanocurcumin, or left untreated as a control. The nanocurcumin formulation (ZALDH-NC) was synthesized and characterized using FTIR, XRD, SEM, and zeta potential analysis to confirm structural integrity and stability. The treated group receiving ZALDH-NC showed a significant reduction in parasite burden compared to other treatments, indicating potent anti-copepod activity. Antioxidant and stress biomarkers, including superoxide dismutase (SOD), catalase (CAT), glutathione (GSH), and total antioxidant capacity (TAC), were significantly improved in the ZALDH-NC group, reflecting a strong oxidative stress response. Additionally, gene expression analyses of proinflammatory cytokines (IL-1β and TNF-α) showed marked upregulation in the ZALDH-NC-treated group, suggesting enhanced immunostimulatory effects. Histopathological evaluation further supported these findings by showing minimal tissue damage and inflammatory infiltration in treated fish compared to the untreated control. These findings demonstrate that Zn Al LDH-nanocurcumin offers improved bioavailability, targeted delivery, and enhanced therapeutic efficacy compared to conventional treatments. Nanocurcumin presents a promising strategy for managing parasitic infections in aquaculture and could contribute significantly to improving fish welfare, production efficiency, and sustainable disease control in aquaculture.

INTRODUCTION

Aquaculture diseases are a major constraint on fish production, causing up to 50% of productivity losses, especially in developing countries **(Assefa & Abunna, 2018)**.

High stocking densities and poor water quality create favorable conditions for the transmission of various pathogens, including parasites **(Lieke *et al*., 2020)**. Parasitic infections not only lead to direct fish mortality but also compromise the host's immune defenses, making them more vulnerable to secondary infections **(Okon *et al*., 2023)**.

One of the most economically significant parasitic diseases in cyprinid fish is lernaeosis, caused by *Lernaea cyprinacea* **(El-Mansy, 2009)**. The common carp (*Cyprinus carpio*), a globally important aquaculture species, is particularly susceptible. It is widely farmed in Asia and Europe due to its commercial and nutritional value **(Winfield & Nelson, 2012; Rahman, 2015)**. However, its production is frequently threatened by various infectious diseases. These include bacterial pathogens such as *Aeromonas hydrophila*, atypical *A. salmonicida*, and *Flavobacterium columnare*; fungal pathogens like *Saprolegnia* spp.; viral infections such as spring viremia of carp (*Rhabdovirus carpio*); and parasites like *Lernaea cyprinacea* **(Bootsma *et al*., 1976; Faisal *et al*., 1988; Abdelgalil *et al*., 2012)**.

The geographic spread of *L. cyprinacea* has expanded to temperate regions, a trend likely driven by climate change and the movement of host species **(Ahnelt *et al*., 2018; Waicheim *et al*., 2019)**. Conventional treatment strategies include chemical, biological, and mechanical methods. However, chemical treatments such as potassium permanganate and organophosphates may not effectively eliminate all life stages of the parasite and could be toxic to fish **(Islam *et al*., 2024)**. Moreover, manual removal is often impractical in large-scale aquaculture operations.

To enhance disease resistance and reduce reliance on chemicals, modern approaches include the use of probiotics, prebiotics, and synbiotics **(Harikrishnan & Balasundaram, 2005; Yilmaz *et al*., 2022)**, along with phytogenic additives. Plant-derived compounds such as grape seed and Cornus mas extracts have shown positive effects on carp growth and immune function **(Mehrinakhi *et al*., 2021; Sadeghi *et al*., 2021; Bakr *et al*., 2024)**, and combinations like *Bacillus licheniformis* with *Citrus aurantifolia* peel have demonstrated antioxidant and immunostimulatory benefits.

Curcumin, the bioactive component of turmeric *(Curcuma longa)*, has been investigated for its antioxidant, anti-inflammatory, antimicrobial, and immunomodulatory activities **(Al-Aameli *et al*., 2020; Pamukçu *et al*., 2022; Şahin *et al*., 2024)**. To improve its bioavailability, researchers have explored nanotechnology-based delivery systems. Dietary nanocomposite of vitamin C and vitamin E enhanced the performance of the Nile tilapia since it helped the fish body scavenge the generated reactive oxidative species **(Sherif *et al*., 2024)**. Moreover, a blend of chitosan-vitamin C and vitamin E nanoparticles robust the immunosuppressed-status in the Nile tilapia treated with salt **(Elnagar *et al*., 2024)**. Further studies illustrated the protective effect of Selenium nanoparticles against Aflatoxicosis in the Nile Tilapia **(Sherif *et al*., 2023)**.

Layered double hydroxides (LDHs), such as zinc–aluminum LDH (Zn/Al LDH), are promising nanocarriers due to their two-dimensional metal hydroxide layers

intercalated with anions, forming a stable three-dimensional structure with high biocompatibility and drug-loading capacity **(Gu *et al*., 2015; Radwan *et al*., 2022)**.

The aim of this study was to evaluate the antiparasitic efficacy of Zn Al LDH loaded with nanocurcumin (ZALDH-NC), commercial *Curcuma longa* (turmeric) and Zn Al LDH (ZA-LDH) against *L. cyprinacea*. Additionally, the study assessed the immunological response of infected fish by analyzing the expression of key cytokines, including interleukins and tumor necrosis factor.

MATERIALS AND METHODS

1. Ethical procedure

This research followed ethical procedures approved by the Institutional Animal Care and Use Committee Faculty of Veterinary Medicine, Beni-Suef University, Egypt. (Approval number 024-041).

2. C. carpio fries

In April 2023, (water temperature 27±2°C), one of the local common carp hatchery fishes' (Abu-Saleh) retailers at Beni-Suef Governorate, Egypt suffered from swollen hyperemic nodules scattered on different parts of the body and open wounds. About 600 common carp fingerlings (5±2g) were captured and transferred alive to the wet lab of Fish Department, Faculty of Veterinary Medicine, Beni-Suef University, Egypt according to **EMEISH (2019)**. Ten glass aquaria of 70 x 25 x 40 cm were supplied with chlorine-free tap water and air supply were used in this work.

3. Clinical examination

C. carpio fries were individually inspected by the naked eye **(Noga, 2010)** for detection of any external gross lesions and/or presence of any parasite.

4. Water quality determination

During the collection of fish samples for examination, water samples were obtained for evaluation of temperature, dissolved oxygen, pH, ammonia, nitrite, sulfate, chloride, and total hardness. The samples were tested in Beni-Suef Drinking Water Central Laboratory by using NIST traceable reference equipment and materials in accordance with ISO/IEC 17025:2005 requirements and the testing methods EBLOW meets ISO/IEC 17025:2005 and accreditation bodies requirements.

5. Parasitological examination and identification

External parasites were examined in all of the fish samples. Samples were measured in triplicate, and the results are presented as the mean ± standard deviation, with 40 specimens per isolate. The identification was based on prior studies **(Ghobashy *et al.*, 2018; Santos *et al.*, 2020)**.

6. Molecular identification

Forty specimens of isolates were washed and cleaned with sterile saline and then preserved at -20°C in an Eppendorf tube. Genomic DNA from cysts was extracted

using the QIAamp DNA Mini kit (Qiagen, Germany) according to the tissue protocol provided by the manufacturer **(Khalifa *et al.*, 2025a)**. The concentration and quality of extracted DNA were determined using the Nanodrop2000 spectrophotometer (NP80, Nanophotometer, Implen, Germany) **(Mahdy *et al.*, 2024a)**. PCR was performed to amplify the cytochrome oxidase subunit I (COXI) gene using the specific degenerate primer pairs; (forward: 5′-TAGTTGGAATTTGGGCTGGC-3′ and reverse: 5′-ATTAGGGGCCTTGTTGGGAAG-3′), that developed by **Hua *et al.* (2019)** and **Behera *et al.* (2022)**. PCR amplifications were performed using Emerald Amp Max PCR Master Mix (Takara, Japan) in a 25µl reaction volume. The thermal cycler was adjusted according to **Ramadan *et al.* (2025a)** with a few alterations. The PCR process started at 94°C/ 2min (initial denaturation) and succeeded by 35 cycles of denaturation at 94°C for 30s, annealing at 50°C for 30s, and extension at 72°C for 1 min, and then ended at 72°C for 10min (final extension). Purification of amplicons was carried out with a QIA quick PCR purification kit (Qiagen, USA) **(Kandil *et al.*, 2020)**. For bidirectional sequencing, PCR products of the COXI gene were submitted with the same primer pairs to Macrogen Inc. (Macrogen, Seol, South Korea) **(Salem *et al.*, 2024a)**. The sequencing process was carried out using the Big Dye terminator cycle sequencing kit, and electrophoresis was accomplished with the 3730XL sequencer model (Applied Biosystems™, USA). The raw data of sequences were edited and assembled using the BioEdit software **(Salem *et al.*, 2023)**. The final sequences were submitted to GenBank to issue the corresponding accession numbers. The assembled sequences were then compared against other sequences using the BLAST program of NCBI **(Ramadan *et al.*, 2025b)**.

7. Scanning electron microscope

The obtained isolates from the studied fishes were carefully rinsed with 0.9% NaCl and preserved with 2.5% glutaraldehyde. They were dehydrated with ethanol ranging from 50 to 100%. The isolates were thoroughly dried with an Autosamdri-815 (Germany) CO_2 critical point dryer. Finally, the isolates were cut at their anterior and posterior ends and bonded to the stub, which was coated with 20nm gold. The copepods were photographed with a scanning electron microscope (JSM 5200, electron probe) and subjected to a micro analyzer (Jeol, Japan) at Cairo University's Faculty of Agriculture.

8. Evaluation of immune response of *C. carpio* to the suspected disease by gene expression

8.1. Assessment of tumor necrosis-α and Interleukin-1β

The skin was collected from the heavily infested fish*;* all samples were aseptically stored at -20°C for subsequent research work **(Salem *et al.*, 2024b)**.

8.1.1. Extraction of RNA

A total mRNA kit (Ambion, Applied Biosystems) was used to extract mRNA from 100mg of infested skin according to the manufacturer's instructions. By using the FastPrep-24 homogenizer (MP Biomedicals, 2 cycles of 30 s at 6 m/s), the skin and gills of fish were homogenized and placed in Lysing Matrix D tubes (MP; Biomedicals). The quantity and purity of mRNA were determined using Nanodrop (Thermo Scientific). According to the manufacturer's recommendations, 500ng of mRNA were obtained using DNaseI amplification grade (Invitrogen). Reverse transcription of the treated RNA was performed using the method described by **(Mahdy *et al.*, 2024b)**, employing the High-Capacity cDNA Archive Kit (Applied Biosystems). Table (1) lists the qRT-PCR primers used for *IL-1β* and *MHC-II*, specifically designed for *Cyprinus carpio* based on sequences deposited in GenBank. Tissue samples were obtained from 1 cm sections of skin and gills infested with *Lernaea cyprinacea*. The procedures for mRNA extraction and cDNA synthesis followed the protocol outlined by **Ramadan *et al.* (2024a)**.

8.1.2. Real-time PCR

The primers for amplifying IL-1β, TNF-α, and β-actin were selected based on published sequences available in GenBank. These primers, validated for *Cyprinus carpio*, target conserved regions to ensure high specificity and efficiency. Each primer set was evaluated via BLAST analysis to confirm target specificity and avoid off-target binding. PCR reactions were optimized using gradient PCR, and an annealing temperature of 60°C was selected based on the primers' melting temperatures (Tm) and GC content.

For quality assurance, all PCR and qPCR assays included appropriate controls. Negative controls (no-template) containing nuclease-free water were included to monitor contamination, and positive controls with DNA templates from healthy *C. carpio* tissue confirmed primer performance. β-actin was used as the housekeeping gene for normalization, and relative expression levels were calculated using the 2^–ΔΔCt method.

The tests were performed on a Step One™ Real-Time PCR System (Applied Biosystems, USA). The reaction mix contained 10µL of SYBR® Premix Ex Taq™ (TliRNase H Plus), ROX Plus (TaKaRa, Japan), 1µL of mDNA, and 0.5µL of the primer (100nM), made up to 20µL with ultra-pure water. Cycling conditions followed those of **Mahdy *et al.* (2024b)**, and ΔCT was calculated by subtracting the β-actin result from the examined gene's result, with ΔCT acting as an internal control.

8.1.3. Conditions for PCR cycling

A 40-cycle amplification protocol was used, consisting of denaturation at 94°C for 30 seconds, annealing at 60°C for 30 seconds, and extension at 72°C for 45 seconds. The real-time PCR technique was developed by **Ramadan *et al.* (2024b, c)**. Samples were collected in triplicate.

Table 1. Primers of the gene expression analysis of the diseased *C. carpio*

Genes	Sequence (5′-3′)	Accession No.	References
Interleukin-1 beta (IL-1β)	F:GATGCGCTGCTCAGCTTCT R:AGTGGGTGCTACATTAACCATACG	AJ249137	**Taha *et al*. (2025)**
Tumor Necrosis Factor alpha (TNF-α)	F:CATTCCTACGGATGGCATTTACTT R:CCTCAGGAATGTCAGTCTTGCAT	EU069817	**Mahdy *et al*. (2024b)**
Beta-Actin (β-Actin) (Housekeeping Gene)	F:GATGCGGAAACTGGAAAGGG R:ATGAGGGCAGAGTGGTAGACG	AB039726	**Salem *et al*. (2024b)**

9. Histopathological examination

Tissue specimens from grossly visible lesions in cutaneous and skeletal muscles were removed and fixed in 10% buffered neutral formalin **(Mahdy & Shaheed, 2001; Suvarna *et al.*, 2018)**. The fixed samples were cleaned, dehydrated, clarified, and paraffin embedded. The paraffin blocks were sectioned at a 5-micron thickness. Hematoxylin and eosin were used to stain the sections according to **Bancroft and Layton (2012)**. Tissue sections were examined in an Olympus BX43 light microscope and captured using an Olympus DP27 camera linked to cellSens dimensions software (Olympus).

10. Treatment trial

10.1. Materials

Zinc chloride hexahydrate ($ZnCl_2 \cdot 6H_2O$) and aluminum chloride hexahydrate ($AlCl_3 \cdot 6H_2O$) were purchased from Chem-Lab (Belgium). Sodium hydroxide (NaOH) and hydrochloric acid (HCl) were obtained from Merck KGaA (Germany). All chemicals used were of analytical grade and high purity. Curcumin (Tur) was sourced from a local supplier in Egypt.

10.2. Synthesis of ZA-LDH and ZA-LDH–NC

According to the method described by **Pavel *et al.* (2020)**, $ZnCl_2 \cdot 6H_2O$ and $AlCl_3 \cdot 6H_2O$ were dissolved in 100mL of distilled water at a Zn:Al molar ratio of 4:1. A 2M NaOH solution was gradually added to the mixture until complete precipitation occurred at pH 8.0. The resulting suspension was stirred at room temperature for 24

hours, then filtered, washed several times with distilled water, and dried at 40 °C for 24 hours.

The LDH nanocomposite (LDH–NC) was synthesized using the same procedure with the addition of curcumin. Specifically, 1.5 grams of Tur were dissolved in 50mL of ethanol and added to the precursor solution before pH adjustment. The Zn:Al:Tur molar ratio was 4:1:0.5. The mixture was stirred for 24 hours at room temperature, followed by filtration, thorough washing, and drying at 40°C.

10.3. Characterization

10.3.1. X-ray diffraction (XRD)

XRD patterns were recorded using a PANalytical Empyrean X-ray diffractometer operating at 40kV and 35mA, utilizing monochromatized Cu Kα radiation (λ = 1.5406 Å). The scan was performed from 5 to 80° (2θ) at a speed of 2°/ min, with a step size of 0.050° and a step time of 1.5 seconds.

10.3.2. Infrared spectroscopy (IR)

Fourier-transform infrared (FTIR) spectra were recorded in the range of 4000–400 cm^{-1} using a Vertex 70 spectrometer (Bruker, Germany). Samples were prepared as KBr pellets. Scans were performed with a resolution of 1 cm^{-1} and averaged over three replicates to identify functional groups present in the samples.

10.4. Hydrodynamic size, polydispersity index (PDI), and ζ–potential analysis

Dynamic light scattering (DLS) was used to determine the hydrodynamic diameter, particle size distribution, and PDI using a ZS90 Zetasizer (Malvern Instruments, UK). ζ–Potential measurements, indicating colloidal stability, were conducted via electrophoretic laser Doppler velocimetry using the same instrument.

10.5. Transmission electron microscopy (TEM)

High-resolution transmission electron microscopy (HRTEM) was employed to observe the surface morphology and particle size of the prepared samples using a JEOL JEM-2100 microscope operating at 200 kV.

10.6. Determination of entrapment efficiency (EE) and loading capacity (LC)

Following curcumin (Tur) loading into Zn–Al LDH, the suspensions were centrifuged at 6000×g for 20 minutes using a Thermo Scientific centrifuge (Waltham, MA, USA) to separate unbound curcumin in the supernatant. The concentration of free curcumin was determined spectrophotometrically using a Thermo Scientific Evolution 600 UV-Vis spectrophotometer (USA) at λmax = 425 nm. Entrapment efficiency (EE) and loading capacity (LC) were calculated based on absorbance measurements, as summarized in Table (2) **(Pavel *et al.*, 2020)**.

Equation (1): $\mathrm{EE}(\%) = \frac{\text{Tur weight in LDH}}{\text{weight of Tur fed initially}} * 100$

Equation (2): $\mathrm{LC}(\%) = \frac{\text{Tur weight in sample}}{\text{total weight of sample}} * 100$

Table 2. Parameters used in determining the EE and LC

Procedure	Equipment	Settings	Purpose
1. Centrifugation of suspensions to separate supernatant containing unbound curcumin (Tur) after loading into Zn Al LDH	Thermo Scientific centrifuge (Waltham, MA, USA)	6,000×g, 20 minutes	To separate unbound Tur from the loaded complex
2. Measurement of free Tur in the supernatant	Thermo Scientific Evolution 600 UV/Vis spectrophotometer (USA)	λmax = 425 nm	To quantify the amount of unbound Tur in the supernatant

10.7. Determination of bioactive compound of Curcumin ((Tur) release)

To study the release pattern of Tur from synthesized Zn Al LDH, 3mg of LDH was incubated in 30mL of 0.1 M phosphate-buffered saline (PBS) at pH 7. The mixture was placed in a dialysis bag with a molecular weight cut-off (MWCO) of 12,000–14,000 Da from Himedia, India, under sink conditions at room temperature and under sunset. These conditions were designed to mimic the environment of water. Samples were taken at predetermined intervals (0, 0.5, 1, 2, 3, 4, 5, 6, 8, 12, 24, and 48hr) **(Pavel *et al.*, 2020)**, with 1mL of dialysate replaced by 1mL of fresh PBS each time. The release of the samples was determined based on their concentration at specific times and the actual Tur content in LDH. The release experiments were conducted three times, and the average results were reported.

10.8. Determination of LC_{50} and LC_{100} of Tur, ZA-LDH and ZALDH-NC on the isolates

The collected isolates were divided into four groups, each group consists of 50 isolate, where group A is subjected to Tur and group B is subjected to ZA-LDH, while group C is subjected to ZALDH-NC at varying concentrations (Table 3). Group D is considered as the control group by immersion of isolates in normal saline. Each concentration was applied in triplicates to tissue culture plates containing the isolates for 10, 20, 30min, and 1 hour. Following removal and preservation in buffered phosphate saline (pH 7.2), all isolates (treated and negative control) were checked at 37^{o}C to see if they were alive or dead **(Mahdy *et al.*, 2023)**. 100% (LC_{100}) and 50% (LC_{50}) lethal quantities were subsequently calculated, according to **Mahdy *et al.***

(2022). The viability of the exposed isolates was ascertained by observing their form and motility under a microscope where dead isolates are immobile.

Table 3. Different concentrations of Tur, ZA-LDH and ZALDH-NC used for the isolates

Substances	Doses
1. Group (A) Tur	150, 300, 450, 600 mg/l
2. Group (B) ZA-LDH	450, 600 mg/l
3. Group (C) ZALDH-NC	50, 75, 100, 200 mg/l

11. Statistical analysis

All data were presented as means ± standard error. **Taha *et al.* (2024a, b)** performed statistical analyses using one-way ANOVA followed by Tukey's post hoc test to assess differences among treatment groups **(Khalifa *et al.*, 2025b)**. All values were expressed as means ± standard error, and statistical significance was set at $P \leq 0.05$ using SPSS (version 27.0 for Windows) **(El Akkad *et al.*, 2022; El-Bahy *et al.*, 2023)**.

RESULTS

Clinical abnormalities of Lernaeosis infested *C. carpio*

As illustrated in Fig. (1), *C. carpio* fingerlings infested with *Lernaea* spp. exhibited prominent clinical signs, including hemorrhagic lesions (hemorrhagic nodules) on the skin and ulcer formation surrounding the attachment sites of the copepods, accompanied by noticeable scale loss. One or more worm-like copepods—gray to greenish in color, with or without paired appendages—were observed firmly attached to the surface of the infected fish. The parasites were distributed across various anatomical regions, including the belly, vent, tail fin, pectoral and dorsal fin bases, and along the body sides.

Fig. 1. Clinical abnormalities of lernaeosis naturally affected cyprinids fingerlings. (A, D) *L. cyprinacea* penetrated the body sides of *C. carpio* fingerlings showing their egg sacs with hyperemic nodules and open wounds. *L. cyprinacea* attachment point around the tail of *C. carpio* fingerlings (c). *C. carpio* fingerlings showed the attachment of more than one *L. cyprinacea* at the caudal peduncle (b)

Water quality

The water temperature, DO, pH, ammonia, nitrite of pond water during lernaeosis examination were 23.3ºC, 6 mg/l, 7.94, 0.02 mg/l, 0.009 mg/l respectively.

Morphological features of *L. cyprinacea*

The female *Lernaea* is characterized by an elongated shape, ranging from 8 to 16mm in length (with an average of 12 ± 1.8 mm). Its front end has an anchor-like structure that penetrates the skin to reach the muscle. This parasite possesses four horns: two dorsal ones that are Y-shaped and two simpler ventral ones. The mouth is situated between the dorsal horns. The body is cylindrical and elongated, leading to a short abdomen that contains two elongated egg sacs, measuring between 2.8 and 4.7 mm (average length of 3.6 ± 0.48mm) (Fig. 2D-E-G-H).

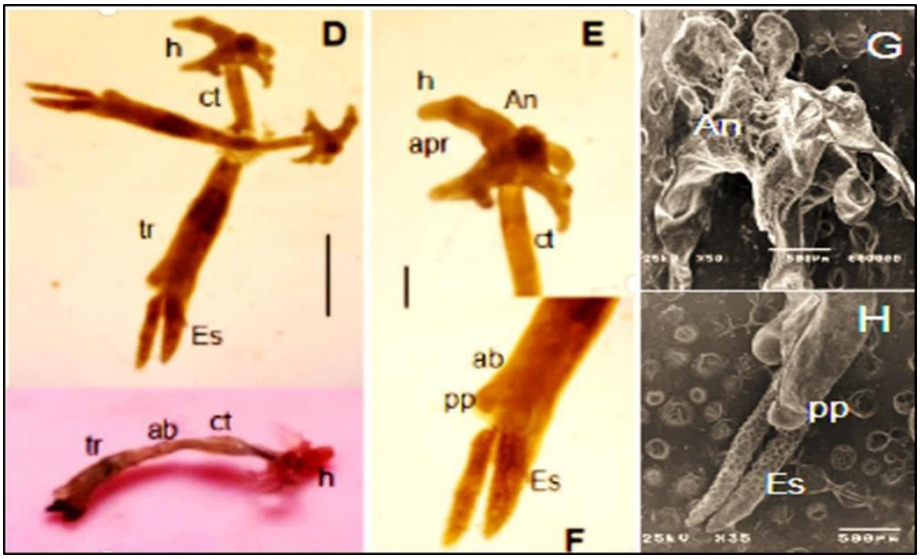

Fig. 2. (D-F) Detail of cephalic structures: apr= anterior protuberance; ppr= posterior protuberance. Scale bare (E)= 3mm.; **(E-F)** = 1mm. G) SEM micrograph of Anterior part of *Lernaea* infested common carp showing anchor= An. **H)** SEM micrograph of posterior part of *Lernaea* infested common carp showing es= egg sac and pp= pregenital prominence

Molecular identification

The PCR products were purified and then bidirectionally sequenced to confirm the identity of the copepod species. The copepod spp. isolates were identified as *L. cyprinacea* (PP421062) depending on alignment-based sequence analysis. In this study, the BLAST analysis of the current *L. cyprinacea* sequence revealed the highest similarity of 100 to 99.28% with other *L. cyprinacea* (OR800156, in India; MH982217 and MK770176 in China; OR431748 in Iraq) sequences available in the GenBank database.

Gene expression of TNF- α and IL-1β in *C. carpio*-infested skin

C. carpio skin infested by *L. cyprinacea*, TNF-α was 20-fold more upregulated than in the control non-infested fish (2.56 ± 0.00) (*P*= 0.0001) (Fig. 3). Concerning the expression of mRNA of IL-1β, it was elevated to 25 folds than control non-infested fish (4.23± 0.00) (*P* = 0.0001) (Fig. 3).

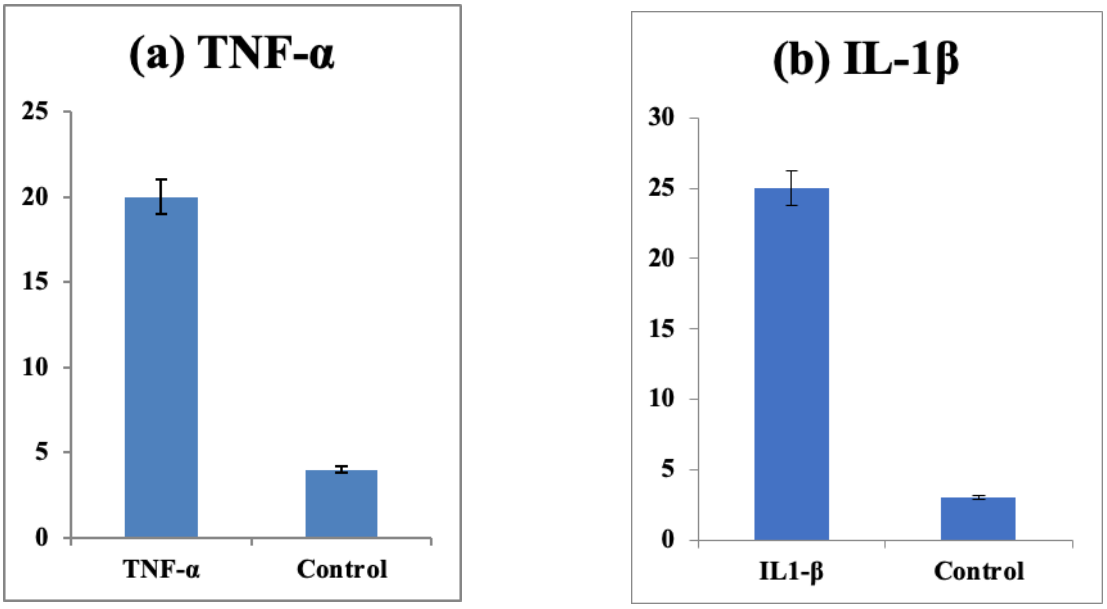

Fig. 3. Immunological expression of (a) TNF-α and (b) IL-Iβ in the skin of infested *C. carpio* with *L. cyprinacea*

Histopathological alterations

Microscopic examination of *C. carpio* tissues infected with *Lernaea cyprinacea* revealed a range of inflammatory reactions affecting both cutaneous and skeletal tissues, varying in severity. Cutaneous lesions involved both the epidermis and dermis. The epidermis exhibited spongiosis and mucous cell hyperplasia, while the dermal layer showed fibrovascular tissue proliferation with angiogenesis and intense infiltration of eosinophilic granular cells (EGCs), indicating areas of healing cutaneous ulceration.

A severe granulomatous reaction was observed in the dermis, with inflammation extending deeply into the underlying skeletal muscle and bony structures. Multiple *L. cyprinacea* parasites were surrounded by intense, multifocal granulomatous inflammation involving skeletal myocytes and osseous tissue. Affected myocytes displayed signs of atrophy, hyaline degeneration, and necrosis, with dense infiltration of EGCs admixed with lymphocytes and melano-macrophages. Bone tissue showed necrosis of osteoid structures accompanied by EGC infiltration. Extensive hemorrhaging was evident in both cutaneous and skeletal tissues (Fig. 4A–I).

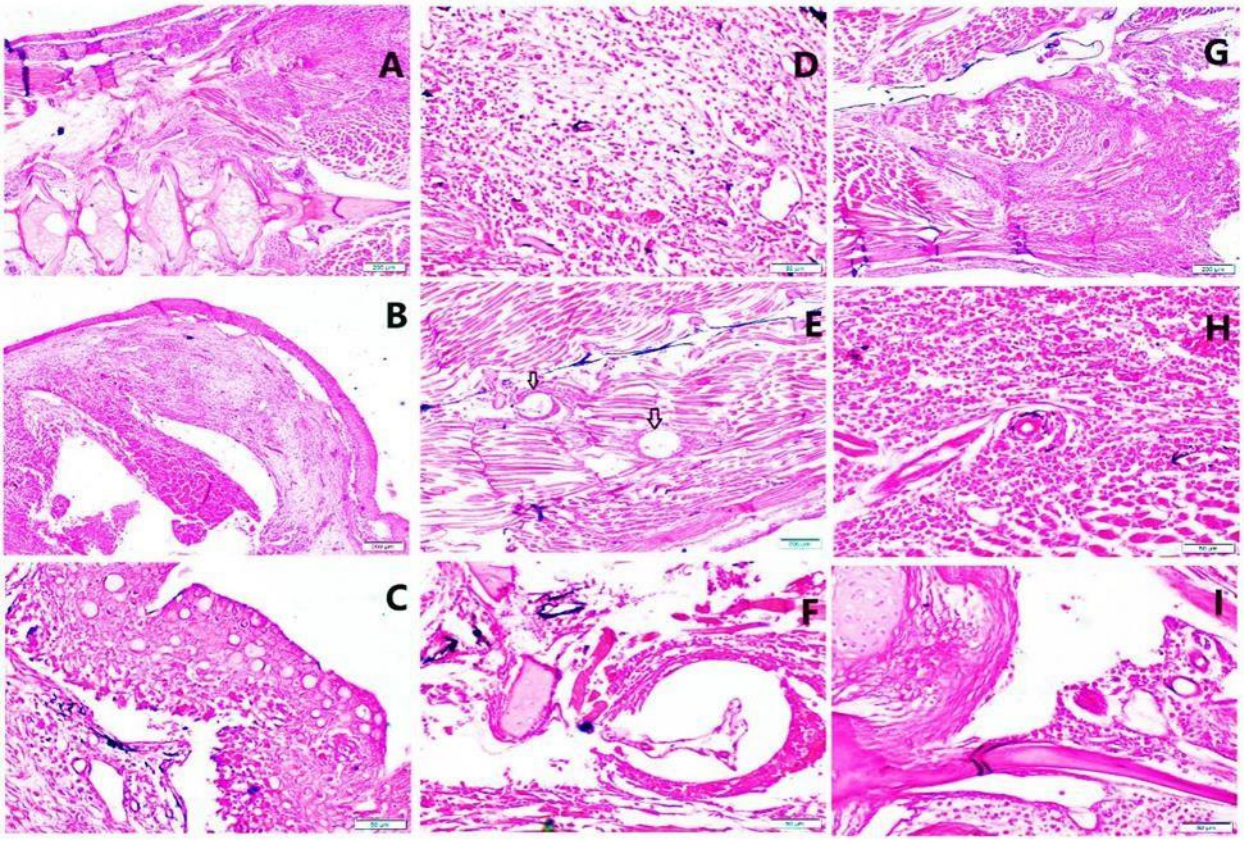

Fig. 4. Photomicrograph of cutaneous and skeletal tissues of crustacean *Lernaea* infected fish showing granulomatous inflammatory reaction involving skin, muscles, and skeletal tissues (A), granulomatous dermatitis with the presence of large granuloma involving the dermal area (B), epidermis showing mucous cell hyperplasia with spongiosis (C), fibrogenesis and angiogenesis of dermis (D), presence of multiple parasites of crustacean *Lernaea* (arrows) deeply embedded in muscle tissue with early granulomatous myositis surrounding them (E), the crustacean *Lernaea* enclosed by delicate capsule and surrounded by EGCs and melano-macrophages aggregation (F), severe granulomatous myositis (G), atrophy, hyaline degeneration and necrosis of muscles with intense EGCs admixed with mononuclear cells infiltrating the muscles (H), necrotic and inflammatory reaction involving the bony tissue (I)

XRD analysis

The X-ray diffraction (XRD) patterns of Zn Al LDH, curcumin (Tur), and ZALDH-NC are presented in Fig. (5). The Zn Al LDH exhibits characteristic sharp and symmetric peaks at 2θ values of approximately 10, 20, and 34°, indicating a well-crystallized layered structure typical of LDHs. Tur displays multiple intense peaks between 10 and 30°, reflecting its crystalline nature. The ZALDH-NC pattern retains the main reflections

of the Zn Al LDH, particularly the basal (003) peak at around 10°, suggesting the preservation of the layered structure after Tur loading. However, the intensity and sharpness of the LDH peaks in ZALDH-NC are reduced compared to pure Zn Al LDH, which may indicate a decrease in crystallinity due to the intercalation process. Notably, the absence of characteristic Tur peaks in the ZALDH-NC pattern suggests that Tur has been successfully intercalated into the LDH interlayers, losing its original crystal structure. The slight shifts and broadening of peaks in the ZALDH-NC pattern, particularly for the (003) reflection, could be attributed to an expansion of the interlayer spacing to accommodate the Tur molecules. These XRD results collectively demonstrate the successful loading of Tur into the Zn Al LDH structure, resulting in a nanocomposite with modified crystalline properties.

FTIR

As shown in Fig. (5), the FTIR spectra of Zn-Al LDH, curcumin (Tur), and ZALDH-NC reveal significant insights into their structural interactions. The Zn Al LDH spectrum shows a broad O-H stretching band at 3455cm^{-1}, indicative of hydroxyl groups and interlayer water, with additional peaks at 1621 and 1363cm^{-1} corresponding to water bending and carbonate anions, respectively. Tur exhibits characteristic peaks at 3485cm^{-1} for O-H stretching, 1614 cm^{-1} and 1500 cm^{-1} for C=C and C=O stretching, and 1274cm^{-1} for C-O stretching. In ZALDH-NC, shifts in curcumin's peaks to 3435, 1619, and 1514cm^{-1} suggest successful incorporation and interaction with the LDH structure, supported by the presence of both curcumin and LDH bands, confirming the formation of a hybrid material with potential enhanced properties.

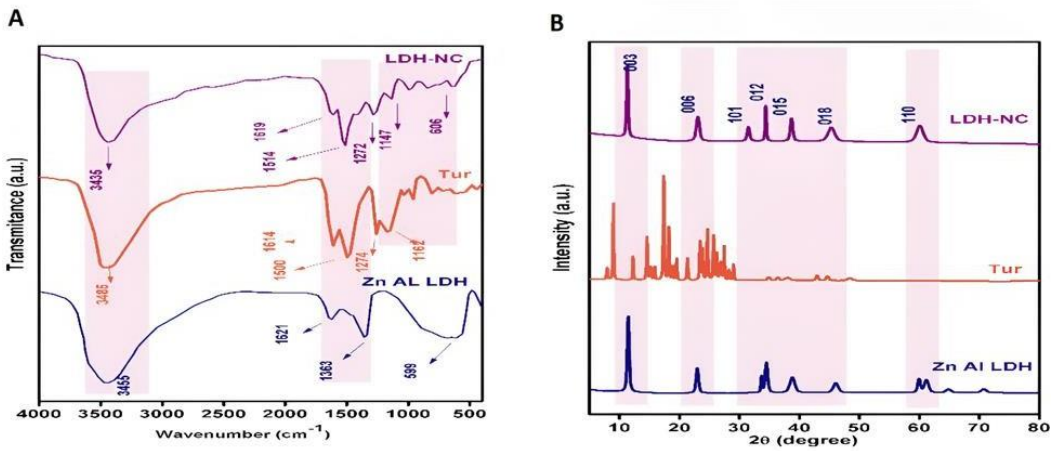

Fig. 5. (A) X-ray diffraction patterns. Inset from 2θ scale within 5-80. (B) FTIR spectra of Zn Al LDH, Tur and ZALDH-NC

DLS and surface charge analysis

As shown in Fig. (6), the zeta size distribution profiles of Zn–Al LDH and ZALDH–NC reveal distinct differences. The Zn–Al LDH sample exhibits a sharp peak centered around 166nm, indicating a narrow and uniform particle size distribution, with a polydispersity index (PDI) of 0.323 ± 0.01. In contrast, the ZALDH–NC sample shows a broader peak centered at approximately 282 nm and a lower PDI of 0.211 ± 0.021, suggesting a larger average particle size and a more heterogeneous distribution. The increased peak intensity for ZALDH–NC may reflect a higher particle concentration or an enhanced scattering effect, likely due to the incorporation of curcumin (Tur), which contributes to particle growth and morphological alteration. This size shift confirms the successful formation of the nanocomposite and may influence its performance in applications requiring tailored material properties.

In terms of surface charge, Zn–Al LDH exhibited a positive zeta potential of 25 ± 1.5 mV, indicating good colloidal stability and a positively charged surface—favorable for interactions with negatively charged biomolecules. In contrast, Tur alone displayed a strongly negative zeta potential of −36 ± 3.4 mV, suggesting excellent dispersion stability due to interparticle repulsion. The ZALDH–NC composite showed a reduced zeta potential of 10 ± 2.3 mV, which points to successful surface interaction between LDH and Tur. The reduction in surface charge likely results from Tur adsorption onto the LDH surface, partially neutralizing the positive charge. While this reduction implies a slight compromise in colloidal stability, it confirms the formation of the composite material.

This interaction between LDH and Tur may enhance the nanocomposite's potential for drug delivery and controlled release, leveraging the structural stability of LDH and the therapeutic bioactivity of Tur. Future investigations could further explore the applicability of ZALDH–NC in pharmaceutical or biomedical domains.

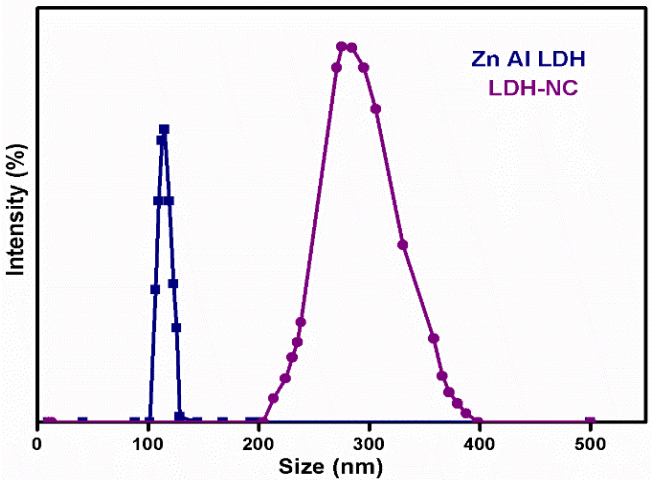

Fig. 6. DLS distribution of Zn Al LDH, Tur and ZALDH-NC

Morphology study

The TEM image of ZALDH–NC (Fig. 7) reveals aggregated nanoparticles exhibiting the characteristic layered morphology typical of layered double hydroxides (LDHs). The observed particles are nanoscale, with an average size of approximately 100 nm, supporting their suitability for applications in nanomedicine. The presence of dense regions within the particles suggests successful loading of curcumin (Tur), which is essential for achieving controlled release and enhanced bioactivity.

This composite structure holds promise for drug delivery systems, as the layered arrangement of LDH can facilitate the sustained release of Tur, potentially improving its therapeutic efficacy. Moreover, the incorporation of zinc may provide synergistic antioxidant effects with Tur, offering additional biomedical advantages. Further investigations into the release kinetics and bioavailability of Tur from the ZALDH–NC composite are warranted to fully elucidate its potential in pharmaceutical and therapeutic applications.

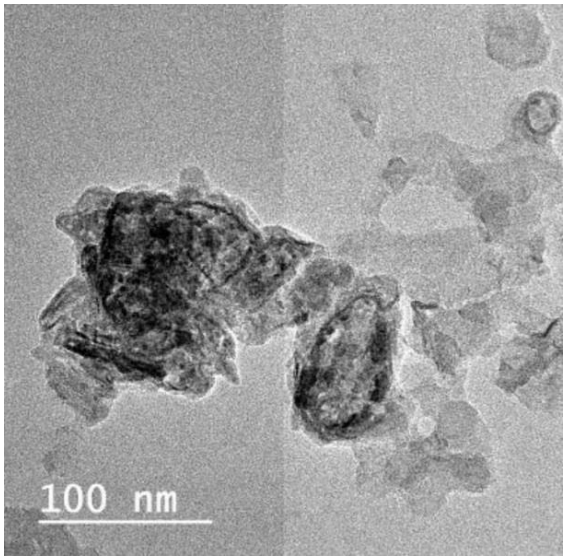

Fig. 7. TEM image of ZALDH-NC

Encapsulation efficiency, Loading capacity and *in vitro* release study

The ZALDH-NC demonstrated a drug loading capacity (LC) of 19.89±2.63% by weight. This formulation achieved a high encapsulation efficiency (EE), successfully incorporating 91.78 ±1.83% of the initial Tur dose into the layered structure. The graph illustrates the cumulative release of curcumin (Tur) under various conditions over time (Fig. 8).

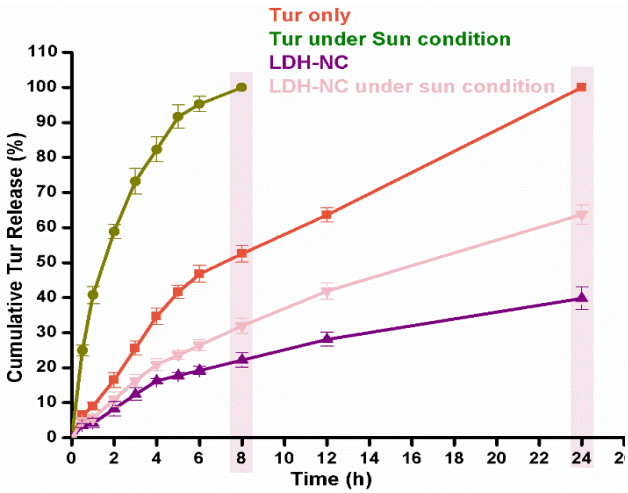

Fig. 8. *In-vitro* curcumin (Tur) release curve from Zn Al LDH

Effects of commercial *Curcuma longa*, ZA-LDH and ZALDH-NC on *L. cyprinacea*

Active, motile *Lernaea cyprinacea* individuals were exposed to commercial *Curcuma longa*, ZA–LDH, and ZALDH–NC at varying concentrations for 10, 20, and 30 minutes, as well as 1 hour. A clear correlation was observed between increasing mortality rates and both concentration and exposure duration for each treatment (Table 4). In all cases, the predicted LC_{50} and LC_{100} values were inversely related to concentration and exposure time—indicating that lower concentrations required longer durations to exert lethal effects.

For *Curcuma longa*, the LC_{50} values were recorded at 300mg/ L (38min) and 450mg/ L (10min), while LC_{100} values were achieved at 450mg/ L (1h) and 600mg/ L (30min and 1h) (Fig. 9). In contrast, ZALDH–NC demonstrated significantly higher potency. The calculated LC_{50} values were 50ppm (28min) and 75ppm (12min), whereas LC_{100} values were achieved at 100ppm (30min and 1h) and 200ppm (20, 30min, and 1h) (Fig. 10).

As shown in Table (3) and Figs. (9, 10), treatment with ZALDH–NC at increasing concentrations resulted in a significantly higher mortality rate of *L. cyprinacea* compared to both *Curcuma longa* and ZA–LDH ($P < 0.05$). Notably, 100% mortality was achieved at lower concentrations and shorter exposure times with ZALDH–NC, confirming its superior antiparasitic efficacy.

Table 4. Number and percentage of mortalities in *L. cyprinacea* subjected to varying doses of commercial *Curcuma longa*, ZA-LDH and ZALDH-NC *in vitro* (n = 50)

Tested concentrations		**Number and mortality rate % of *L. cyprinacea* after exposure to**			
		10min.	**20min.**	**30min.**	**1hr.**
Group (A) commercial *Curcuma longa*	150mg/l	3/6%^{d}	6/12%^{d}	12/ 24%^{c}	21/42%^{ab}
	300mg/l	9/18%^{c}	16/32%^{b}	23/46%^{a}	33/66%^{a}
	450mg/l	25/50%^{bc}	36/72%^{ab}	42/84%^{a}	50/100%^{a}
	600mg/l	33/66%^{ab}	42/84%^{a}	50/100%^{a}	50/100%^{a}
Group (B) ZA-LDH	450mg/l	0.0	0.0	4/8%^{d}	8/16%^{d}
	600mg/l	0.0	5/10%^{d}	9/18%^{d}	14/28%^{d}
Group (C) ZALDH-NC	50 ppm	6/12%^{d}	13/26%^{d}	27/54%^{c}	39/78%^{ab}
	75 ppm	23/46%^{c}	31/62%^{b}	40/80%^{a}	49/98%^{a}
	100 ppm	33/66%^{bc}	46/92%^{ab}	50/100%^{a}	50/100%^{a}
	200 ppm	44/88%^{ab}	50/100%^{a}	50/100%^{a}	50/100%^{a}
Group (D)	Control in saline	0.0	0.0	0.0	4/8%^{d}

Data represented as the mean of triplicates, a column with different letters are statistically significant at $P \leq 0.05$ (One-way ANOVA).

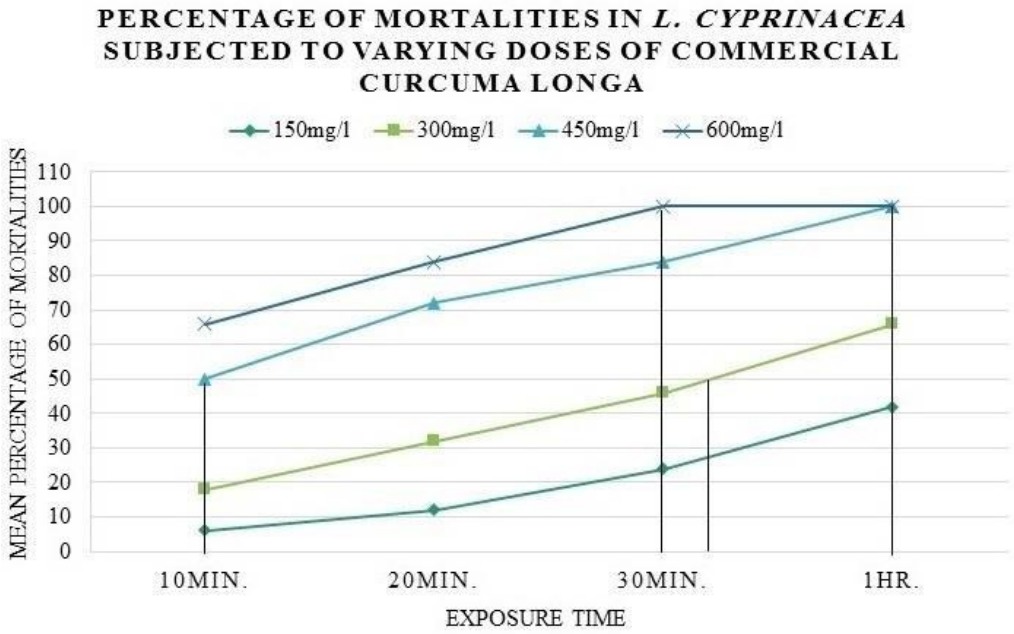

Fig. 9. Percentage of mortalities in *L. cyprinacea* subjected to varying doses of commercial *Curcuma longa*

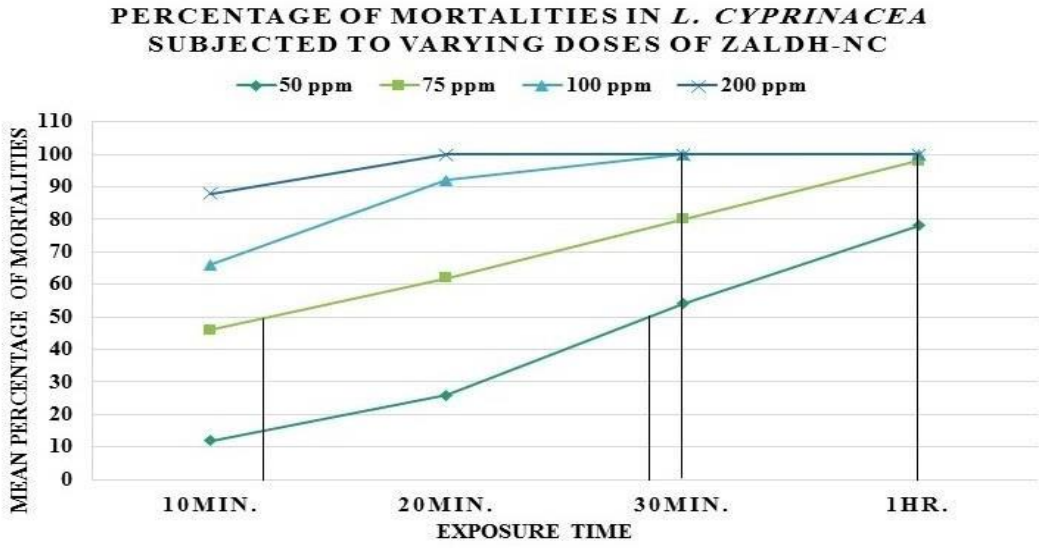

Fig. 10. Percentage of mortalities in *L. cyprinacea* subjected to varying doses of ZALDH-NC

DISCUSSION

Despite recent advancements, controlling major parasitic diseases in aquaculture remains a persistent challenge, requiring increased oversight and innovation. The growing importance of aquaculture has amplified concerns about parasitic infections and their detrimental effects on fish health and reproductive capacity **(Novakov *et al.*, 2015)**. Among these, lernaeosis—caused by *Lernaea cyprinacea*—poses a significant threat to global aquaculture, particularly under suboptimal water conditions, where it compromises fish immunity **(Ageng'o *et al.*, 2024)**. This parasite attaches to the skin of *Cyprinus carpio*, causing blood and mucus loss, tissue damage, and elevated mortality rates, especially in juvenile fish. In the present study, clinical signs included the presence of gray-green copepods attached to hemorrhagic nodules, consistent with previous reports **(Abdelgalil *et al.*, 2012; El-Deen *et al.*, 2013; Fatma, 2014)**.

Environmental conditions such as water temperature and dissolved oxygen (DO) levels play a critical role in the severity of parasitic outbreaks. Lernaeosis is known to proliferate in cooler water (13–23 °C) **(Bilal *et al.*, 2021)**. Our results corroborate these findings, revealing a correlation between temperature fluctuations, increased DO, and parasite intensity, aligning with earlier observations **(Barson *et al.*, 2008)**.

Morphological identification of *L. cyprinacea* traditionally relies on variations in the anchor structure, which may differ based on host species and attachment site. To resolve taxonomic ambiguity, COXI gene sequencing was employed and confirmed the parasite's identity in this study **(Hua *et al.*, 2019)**.

Fish are known to mount immune responses against parasitic infections **(Zhou *et al.*, 2018)**. In our study, infected gill, skin, and mucus samples from *C. carpio* exhibited significant upregulation of pro-inflammatory cytokines *TNF-α* and *IL-1β*, indicating activation of innate immune pathways. These results support the key role of *IL-1β* in host defense **(Dinarello, 2011)**.

Histopathological analyses revealed granulomatous inflammation and necrosis in parasitized muscle tissues, further highlighting the invasive nature of *L. cyprinacea* and its harmful effects—consistent with earlier reports **(Bednarska *et al.*, 2009)**.

The use of dietary nanomaterials such as zinc oxide and titanium dioxide to enhance immune response and disease resistance in Nile tilapia has been extensively documented **(Sherif *et al.*, 2022; 2023; Sherif & Zommara, 2024)**. Curcumin, the principal polyphenol in turmeric, has also gained attention as a functional feed additive in aquaculture **(Al-Aameli *et al.*, 2020; Krishnaveni *et al.*, 2023; Altun *et al.*, 2024)**. A comparative study by **Eissa *et al.* (2024)** demonstrated the superior performance of nanocurcumin (NCur) over free curcumin and Cur/NCur blends in the red tilapia. Similarly, our findings confirmed that Zn–Al LDH–nanocurcumin (ZALDH–NC) exhibited significantly greater antiparasitic efficacy ($P < 0.05$) than both commercial *Curcuma longa* and ZA–LDH at all tested concentrations.

Structural characterization using XRD and FTIR confirmed successful intercalation of curcumin into the Zn–Al LDH matrix, forming a stable nanocomposite with enhanced properties **(Kovalenko *et al.*, 2022)**. Zeta potential analysis further demonstrated good colloidal stability and favorable interaction between components, supporting a controlled release profile and improved therapeutic potential **(Li *et al.*, 2005)**.

In release profile studies, free curcumin exhibited rapid initial release, while ZALDH–NC showed a slower, sustained release pattern—indicating improved bioavailability and physicochemical stability **(Pavel *et al.*, 2020)**. This controlled release mechanism is critical for maximizing curcumin's therapeutic efficacy over extended periods.

In conclusion, our findings confirm that *L. cyprinacea* infestations can be effectively managed using ZALDH–NC, which demonstrated the highest antiparasitic activity, followed by commercial *Curcuma longa*. These results, supported by prior studies **(Shahiduzzaman *et al.*, 2011; Cervantes-Valencia *et al.*, 2019; Abdelhiee *et al.*, 2025)**, highlight nanocurcumin's promise as a next-generation antiparasitic agent. Compared to conventional treatments, nanocurcumin offers superior stability, enhanced bioavailability, and prolonged efficacy—making it a compelling candidate for integrated parasite management strategies in aquaculture.

CONCLUSION

In conclusion, effective control of lernaeosis is essential for improving fish health, maximizing economic returns, and ensuring the long-term sustainability of the aquaculture industry. The development of Zn–Al LDH–nanocurcumin has demonstrated promising antiparasitic activity, particularly against *Lernaea cyprinacea*. This nanocomposite formulation exhibits enhanced bioavailability, targeted delivery, and improved therapeutic efficacy, making it a strong candidate for the management of parasitic infections in aquaculture.

Raising awareness among fish farmers, promoting best management practices, and implementing proper control measures are critical steps toward reducing the prevalence and impact of lernaeosis. Based on these promising in vitro results, further in vivo studies are strongly recommended to evaluate the safety and effectiveness of these natural, environmentally friendly formulations under practical farming conditions.

REFERENCES

Abdelgalil, M.; Essa, M. A and Korni, F. (2012). Studies on Lernaeosis and the efficacy of Dipterex as treatment in the Hatchery Reared Fingerlings of Cyprinids. J. Am. Sci., 8: 5744-5580.

Abdelhiee, E.Y.; Fadl, S.E.; Ashry, A.; Eid, M.M.; Eltholoth, M.M.; Anas, N.; Abdelghany, A.S. and Aboubakr, M. (2025). Harnessing Nature: The Role of Medicinal Plants in Alleviating Cisplatin Toxicity.

Ageng'o, F.O.; Waruiru, R.M.; Wanja, D.W.; Nyaga, P.N.; Hamisi, M.M.; Khasake, C.N.; Wainaina, J.M.; Munde, B.M.; Mbuthia, P.G. and Kamuti, N.M. (2024). Relationship between Water Quality Parameters and Parasite Infestation in Farmed *Oreochromis niloticus* in Selected Rift Valley Counties, Kenya. Aquac. Res., 1: 6139798.

Ahnelt, H.; Konecny, R.; Gabriel, A.; Bauer, A.; Pompei, L.; Lorenzoni, M. and Sattmann, H. (2018). First report of the parasitic copepod *Lernaea cyprinacea* (Copepoda: Lernaeidae) on gobioid fishes (Teleostei: Gobonellidae) in southern Europe. Knowledge & Management of Aquatic Ecosystems, 419: 34.

Al-Aameli, M. H.; Al-Taee, R. A. M. and Kadhim, K. S. (2020). Histological and Physiological Effect of Turmeric (*Curcuma Longa*) on Liver, Pancreas and Kidney. Medico-Legal Update, 20(4).

Altun, G.; Almasaad, J.; Tunalı, M.B.; Tüfekci, K.K. and Kaplan, S. (2024). Promising Effects of Curcumin on Axon Morphology in A Streptozotocin-Induced Diabetic Female Rat Model: Responses to Early, Simultaneous, And Late Treatments. Pak Vet J., 2025, 45(1): 344-351.

Assefa, A. and Abunna, F. (2018). Maintenance of fish health in aquaculture: review of epidemiological approaches for prevention and control of infectious disease of fish. Vet. Med. Int., 2018(1): 5432497.

Bakr, A.F.; Youssef, F.S.; Bahr, A.D. and Ramadan, R.M. (2024). Health Benefits of Astragalus Polysaccharides and Possible Techniques for Upgrading Their Efficiency: A Comprehensive Review. Egypt J. Chem., 67(11): 29-44.

Bancroft, J. D. and Layton, C. (2012). The hematoxylins and eosin. Bancroft's theory and practice of histological techniques, 173-186.

Barson, M.; Mulonga, A. and Nhiwatiwa, T. (2008). Investigation of a parasitic outbreak of *Lernaea cyprinacea* Linnaeus (Crustacea: Copepoda) in fish from Zimbabwe. Afri. Zool., 43(2): 175-183.

Bednarska, M.; Bednarski, M.; Sołtysiak, Z. and Polechoński, R. (2009). Invasion of *Lernaea cyprinacea* in rainbow trout (*Oncorhynchus mykiss*). Acta Sci. Pol., Medicina Veterinaria 8(4) 2009: 27-32

Behera, B. K.; Dhar, S.; Kumar, V.; Parida, P.K.; Hoque, F.; Parida, S.N.; Bisai, K.; Devnath, S.; Jana, A.K.; Mistri, A. and Kumar, B. (2022). Molecular approach and techniques used in the diagnosis of fish parasites. AATCC Review (2022): 34-54.

Bilal, M.; Abbas, F.; Atique, U.; Rehman, M.H.U.; Inayat, M.; Zohaib, M.; Saleem, M.; Fatima, S.; Sherazi, S.W.S.M.; Tehreem, A. and Ali, A. (2021). Lernaeid parasites prevalence in commercial freshwater fish species at various fish farms in Pakistan. Braz. J. Biol., 84, e253868.

Bootsma, R. and Clerx, J.P.M. (1976). Columnaris disease of cultured carp Cyprinus carpio L. Characterization of the causative agent. Aquac., *7*(4): 371-384.

Cervantes-Valencia, M.E.; Hermosilla, C.; Alcalá-Canto, Y.; Tapia, G.; Taubert, A. and Silva, L. M. (2019). Antiparasitic efficacy of curcumin against *Besnoitia besnoiti* tachyzoites *in vitro*. Front. Vet. Sci., (5): 333.

Dinarello, C.A. (2011). Interleukin-1 in the pathogenesis and treatment of inflammatory diseases. Blood. The Journal of the American Society of Hematology, 117(14): 3720-3732.

Eissa, E.-S. H.; Hendam, B. M.; Dighiesh, H.S.; Abd Elnabi, H.E.; Abd El-Aziz, Y. M.; Eissa, M. E.; Abdelnour, S. A. and Ghanem, S.F. (2024). Comparative effects of curcumin, nano curcumin and their combination on reproductive traits and spawning performance of red tilapia (*Oreochromis Niloticus* X *O. Mossambicus*). BMC Veterinary Research, 20(1): 427.

El Akkad, D.M.; Ramadan, R.M.; Auda, H.M.; Abd El-Hafez, Y.N.; El-Bahy, M.M. and Abdel-Radi, S. (2022). Improved dot-ELISA assay using purified sheep *Coenurus cerebralis* antigenic fractions for the diagnosis of zoonotic coenurosis. World's Vet. J., (3): 237-249.

El-Bahy, M.M.; Kamel, N.O.; Auda, H.M. and Ramadan, R.M. (2023). A smart economic way to control camel parasites and improve camel production in Egypt. Expe. Parasitol., (255): 108650.

El-Deen, A.I.E.; Azza, H.M.H. and Abeer, E.M. (2013). Studies on Lernaeosis affecting cultured golden fish (*Carassius auratus*) and trail for its treatment in earthen ponds at Kafr El-Sheikh governorate, Egypt. Global Veterinaria (11): 521-527.

El-Mansy, A. (2009). On the occurrence of adult females of lernaea species (Crustacea:Copepoda) parasitic on goldfish *Carassius auratus (Linnaeus)* in some commercial aquaria in Egypt. Egypt. J. Aquat. Biol. Fish., 13(1): 7-63.

Elnagar, M. A.; Khalil, R.H.; Talaat, T.S. and Sherif, A.H. (2024). A blend of chitosan-vitamin C and vitamin E nanoparticles robust the immunosuppressed-status in N. tilapia treated with salt. BMC Vete. Res., 20(1): 331.

EMEISH, W. (2019). ADAPTATION OF COMMON CARP TO SALINITY. Assiut Vet. Med. J., 65(162): 101-110.

Faisal, M.; Easa, M.e.-S.; Shalaby, S. and Ibrahim, M. (1988). Epizootics of *Lernaea cyprinacea* (Copepoda: Lernaeidae) in imported cyprinids to Egypt. Der Tropenlandwirt-Journal of Agriculture in the Tropics and Subtropics 89(2): 131-141.

Fatma, M. (2014). Lernaeosis affecting hatchery reared common carp (*Cyprinus carpio*) fries and a novel approach for its treatment. Global Journal of Fisheries and Aquaculture Res., 1(2): 173 -189

Ghobashy, M.; Abou Shafeey, H. and Taeleb, A. (2018). Guppy (Poecilia) Poeciliidae fish naturally infected with *Lernaea cyprinacea* parasites (Linnaeus 1758) in KSA. Parasitol. United J., 11(3): 141-148.

Gu, Z.; Atherton, J. J. and Xu, Z. P. (2015). Hierarchical layered double hydroxide nanocomposites: structure, synthesis and applications. Chemical Communications 51(15): 3024-3036.

Harikrishnan, R. and Balasundaram, C. (2005). Modern trends in Aeromonas hydrophila disease management with fish. Rev. Fish. Sci., 13(4): 281-320.

Hua, C.J.; Zhang, D.; Zou, H.; Li, M.; Jakovlić, I.; Wu, S.G.; Wang, G.T. and Li, W.X. (2019). Morphology is not a reliable taxonomic tool for the genus Lernaea: molecular data and experimental infection reveal that *L. cyprinacea* and *L. cruciata* are conspecific. Parasit. vectors, (12): 1-13.

Islam, S.I.; Rodkhum, C. and Taweethavonsawat, P. (2024). An overview of parasitic co-infections in tilapia culture. Aquac. Int., 32(1): 899-927.

Kandil, O.M.; Abdelrahman, K.A.; Mahmoud, M.S.; Mahdy, O.A.; Ata, E.B.; Aloufi, A.S. and Al-Olayan, E. (2020). Cystic echinococcosis: development of an intermediate host rabbit model for using in vaccination studies. Exp. Parasitol., 208, p.107800.

Khalifa, M.M.; Salem, M.A.; Fouad, E.A.; Bakry, N.M.; Kamel, M.S.; El-Bahy, M.M. and Ramadan, R.M.; (2025a). Vector-borne pathogens in dogs in Egypt: Molecular and immunological insights. Res. Vet. Sci., p.105629.

Khalifa, M.M.; Mohamed, H.I.; Ramadan, R.M.; Youssef, F.S.; El-Bahy, M.M. and Abdel-Radi, S. (2025b). Smart application of silver nanoparticles in the treatment of chicken coccidiosis in combination with special supplement to alleviate its toxicity. Vet. Parasitol., 336, p.110440.

Kovalenko, V.; Borysenko, A.; Kotok, V.; Nafeev, R.; Verbitskiy, V.; and Melnyk, O. (2022). Determination of the dependence of the structure of Zn-Al layered double hydroxides, as a matrix for functional anions intercalation, on synthesis conditions. *Eastern-European Journal of Enterprise Technologies*.

Krishnaveni, P.; Thangapandiyan, M.; Raja, P. and Rao, G.V.S. (2023). Pathological and molecular studies on antitumor effect of curcumin and curcumin solid lipid nanoparticles. Pakist. Vet. J., 43(2).

Li, S.; Xu, J.; Zhao, G.; and Chen, H. (2005). Influence of Molar Ratio of Zn/Al/Tyr on the Formation of Tyr/Zn-Al-LDH Nanohybrids. *Chinese Journal of Chemistry*, (23): 1343-1347.

Lieke, T.; Meinelt, T.; Hoseinifar, S.H.; Pan, B.; Straus, D.L. and Steinberg, C.E. (2020). Sustainable aquaculture requires environmental-friendly treatment strategies for fish diseases. Rev. Aquac., 12(2): 943-965.

Mahdy, O.A. and Shaheed, I.B. (2001). Studies on metacercarial infection among Tilapia species in Egypt. Helminthologia, (38):1, 35-42.

Mahdy, O. A.; Abdel-Maogood, S. Z.; Abdelrahman, H. A.; Fathy, F. M. and Salem, M. A. (2022). Assessment of *Verbesina alternifolia* and *Mentha piperita* oil extracts

on *Clinostomum phalacrocoracis* metacercariae from Tilapia zillii. Beni -Suef University Journal of Basic Applied Sciences, 11(1), 48.

Mahdy, O. A.; Abdelsalam, M. and Salem, M. A. (2023). Molecular characterization and immunological approaches associated with yellow grub trematode (*Clinostomid*) infecting Nile Tilapia. Aquac. Res., https://doi.org/10.1155/2023/5579508.

Mahdy, O.A.; Abdel-Maogood, S.Z.; Abdelsalam, M. and Salem, M.A. (2024a). A multidisciplinary study on Clinostomum infections in Nile tilapia: micro-morphology, oxidative stress, immunology, and histopathology. BMC Veterinary Research, 20(1): 60.

Mahdy, O. A.; Mai, A.S, Mohamed Abdelsalam, Shaheed, I.B.; and Attia, M.M. (2024b). Immunological and molecular evaluation of zoonotic metacercarial infection in freshwater fish: A cross-sectional analysis, Res. Vet. Sci., 172,105239, ISSN 0034-5288.

Mehrinakhi, Z.; Ahmadifar, E.; Sheikhzadeh, N.; Moghadam, M.S. and Dawood, M.A. (2021). Extract of grape seed enhances the growth performance, humoral and mucosal immunity, and resistance of common carp (*Cyprinus carpio*) against *Aeromonas hydrophila*. Annals of Animal Science, 21(1), pp.217-232.

Noga, E. J. (2010). Fish disease: diagnosis and treatment, John Wiley & Sons.

Novakov, N.; M. Ćirković, B. Kartalović, M. Pelić, D. Matić, D. Ljubojević and B. Božić (2015). Infestation of *Larnaea cyprinacea* (Crustacea: Cepopoda) in different categories of common carp (*Cyprinus carpio*) reared in Serbia. Archives of Veterinary Medicine, 8(2): 11-18.

Okon, E. M.; Okocha, R. C., Taiwo A. B., F. B. Michael and A. M. Bolanle (2023). Dynamics of co-infection in fish: A review of pathogen-host interaction and clinical outcome. Fish Shellfish Immunol Rep., 4: 100096.

Pamukçu, A.; Erdoğan, N.; Şen Karaman, D. (2022). Polyethylenimine-grafted mesoporous silica nanocarriers markedly enhance the bactericidal effect of curcumin against *Staphylococcus aureus* biofilm. Journal of Biomedical Materials Research Part B: Applied Biomaterials, 110(11): 2506-2520.

Pavel, O. D.; Şerban, A.; Zăvoianu, R.; Bacalum, E. and Bîrjega, R. (2020). Curcumin Incorporation into Zn3Al Layered Double Hydroxides—Preparation, Characterization and Curcumin Release. Crystals 10(4): 244.

Radwan, I. T.; Baz, M. M.; Khater, H.; Alkhaibari, A. M. and Selim, A. M. (2022). Mg-LDH nanoclays intercalated fennel and green tea active ingredient: Field and laboratory evaluation of insecticidal activities against Culex pipiens and their non-target organisms. Molecules, 27(8), 2424.

Rahman, M. M. (2015). Role of common carp (*Cyprinus carpio*) in aquaculture production systems. Frontiers in Life Science, 8(4): 399-410.

Ramadan, R. M.; Bakr, A. F.; Fouad, E.; Mohammed, F. F.; Abdel-Wahab, A. M.; Abdel-Maogood, S. Z. and Salem, M. A. (2024a). Novel insights into antioxidant

status, gene expression, and immunohistochemistry in an animal model infected with camel-derived *Trypanosoma evansi* and *Theileria annulata*. Parasites & Vectors, 17(1), 474.

Ramadan, R. M.; Mahdy, O. A.; El-Saied, M. A.; Mohammed, F. F. and Salem, M. A. (2024b). Novel insights into immune stress markers associated with myxosporeans gill infection in Nile tilapia (molecular and immunohistochemical studies). Plos one, 19(6): e0303702.

Ramadan, R. M.; Taha, N. M.; Auda, H. M.; Elsamman, E. M.; El-Bahy, M. M. and Salem, M. A. (2024c). Molecular and immunological studies on Theileria equi and its vector in Egypt. Experimental and Applied Acarology, 93(2): 439-458.

Ramadan, R.M.; Wahby, A.M.; Bakry, N.M.; Auda, H.M.; Mohammed, F.F.; El-Bahy, M.M. and Hekal, S.H.A. (2025a). Targeted pre-partum strategies to suppress *Toxocara vitulorum hypobiotic* larvae: reducing transmission to calves and genotypic insights into Buffalo infections. Veterinary World, 18(2), 329.

Ramadan, R. M.; Salem, M. A.; Mohamed, H. I.; Orabi, A.; El-Bahy, M. M. and Taha, N. M. (2025b). *Dermanyssus gallinae* as a pathogen vector: Phylogenetic analysis and associated health risks in pigeons. Veterinary Parasitology: Regional Studies and Reports, 101198.

Sadeghi, F.; Ahmadifar, E.; Shahriari, M.M.; Ghiyasi, M.; Dawood, M.A.O. and Yilmaz, S. (2021). Lemon, *Citrus aurantifolia*, peel and *Bacillus licheniformis* protected common carp, *Cyprinus carpio*, from *Aeromonas hydrophila* infection by improving the humoral and skin mucosal immunity, and antioxidative responses." Journal of the World Aquaculture Society 52, no. 1: 124-137.

Şahin, İ.O.; Tunalı, M.B.; Aktaş, A.; Tüfekci, K.K. and Kaplan, S. (2024). The Effects of Curcumin on Hyperglycaemia-Induced Optic Nerve Damage in Wistar Albino Rats: An Electron Microscopic and Stereological Study. Pakistan Veterinary Journal, 44(4).

Salem, M. A.; Mahdy, O. A.; Shaalan, M. and Ramadan, R. M. (2023). The phylogenetic position and analysis of Renicola and Apharyngostrigea species isolated from Cattle Egret (*Bubulcus ibis*). Scientific Reports, 13(1): 16195.

Salem, M. A.; Taha, N. M.; El-Bahy, M. M. and Ramadan, R. M. (2024a). The Phylogenetic position of the pigeon mite, *Ornithonyssus sylviarum*, with amplification of its immunogenetic biomarkers in Egypt. Sci Rep 14, 22026.

Salem, M. A.; Mahdy, O. A.; Ramadan, R. M. (2024b). Ultra-structure, genetic characterization and Immunological approach of fish borne zoonotic trematodes (Family: *Heterophyidae*) of a redbelly tilapia. Research in Veterinary Science. Vol. 166, January 2024, 105097.

Santos, E. L.; De Jesus Silva, T.; De Lima, M. R.; Junior, R. F. T. C.; Da Silva, S. J. C. and Soares, E. C. (2020). First record of *Lernaea cyprinacea* (*Linnaeus*,

1758)(Copepoda: Cyclopoida) on Betta splendens in Brazil. Revista Principia-Divulgação Científica e Tecnológica do IFPB, 50:155-167.

Shahiduzzaman, M. D. and Daugschies, A. (2011). Curcumin: a natural herb extract with antiparasitic properties. Nature Helps... How Plants and Other Organisms Contribute to Solve Health Problems, 141-152.

Sherif, A. H.; Khalil, R. H.; Tanekhy, M.; Sabry, N. M.; Harfoush, M. A. and Elnagar, M. A. (2022). *Lactobacillus plantarum* ameliorates the immunological impacts of titanium dioxide nanoparticles (rutile) in *Oreochromis niloticus*. Aquac. Res. 53: 3736–3747. https://doi.org/10.1111/are.15877

Sherif, A.H. and Zommara, M. A. (2024). Selenium Nanoparticles Ameliorate Adverse Impacts of Aflatoxin in Nile Tilapia with Special Reference to Streptococcus agalactiae Infection. Biol. Trace Elem. Res. 202(10): 4767-4777. https://doi.org/10.1007/s12011-023-04031-1

Sherif, A.H.; Elkasef, M.; Mahfouz, M.E. and Kasem E.A. (2023). Impacts of dietary zinc oxide nanoparticles on the growth and immunity of Nile tilapia could be ameliorated using *Nigella sativa* oil. J. Trace Elem. Med. Biol, 79 (2023): 127265. https://doi.org/10.1016/j.jtemb.2023.127265

Sherif, A.H.; Khalil, R. H.; Talaat, T. S.; Baromh, M. Z. and Elnagar, M. A. (2024). Dietary nanocomposite of vitamin C and vitamin E enhanced the performance of Nile tilapia. Sci, Rep., 14(1): 15648. https://doi.org/10.1038/s41598-024-65507-1

Suvarna, S. K.; Layton, C.; Bancroft, J. D. (2018). Bancroft's Theory and Practice of Histological Techniques, Eighth Edition, pp. 1–557.2018, ISBN,978-070206887- 4, 978-070206864-5

Taha, N. M.; Sabry, M. A.; El-Bahy, M. M. and Ramadan, R. M. (2024a). Awareness of parasitic zoonotic diseases among pet owners in Cairo, Egypt. Veterinary Parasitology: Regional Studies and Reports, 51, p.101025.

Taha, N. M.; Youssef, F. S.; Auda, H. M.; El-Bahy, M. M. and Ramadan, R. M. (2024b). Efficacy of silver nanoparticles against *Trichinella spiralis* in mice and the role of multivitamin in alleviating its toxicity. Scientific Reports, 14(1): 5843.

Taha, N.M.; Salem, M.A.; El-Saied, M.A.; Mohammed, F.F.; Kamel, M.; El-Bahy, M.M. and Ramadan, R.M. (2025). Multifaceted analysis of equine cystic echinococcosis: genotyping, immunopathology, and screening of repurposed drugs against *E. equinus protoscolices*. BMC Veterinary Research, 21(1), p.178.

Waicheim, M. A.; Arbetman, M. P.; Rauque Perez, C. A. and Viozzi, G. P. (2019). The invasive parasitic copepod *Lernaea cyprinacea*: updated host-list and distribution, molecular identification and infection rates in Patagonia.

Winfield, I. J. and Nelson, J. S. (2012). Cyprinid fishes: systematics, biology and exploitation, Springer Science & Business Media.

Yilmaz, S.; Yilmaz, E.; Dawood, M.A.; Ringø, E.; Ahmadifar, E. and Abdel-Latif, H.M. (2022). Probiotics, prebiotics, and synbiotics used to control vibriosis in fish: A review. Aquaculture, 547, p.737514.

Zhou, S.; Li, W. X.; Zou, H.; Zhang, J.; Wu, S. G.; Li, M. and Wang, G. T. (2018). Expression analysis of immune genes in goldfish (*Carassius auratus*) infected with the monogenean parasite *Gyrodactylus kobayashii*. Fish Shellfish. Immunol.; 77: 40-45.